Title

An Innovative Nanobody-Based Electrochemical Immunosensor Using Decorated Nylon Nanofibers for Point-of-Care Monitoring of Human Exposure to Pyrethroid Insecticides

Journal

ACS Applied Materials & Interfaces, 12(5)

ISSN

1944-8244

Authors

El-Moghazy, Ahmed Y

Huo, Jingqian

Amaly, Noha

et al.

Publication Date

2020-02-05

DOI

10.1021/acsami.9b16193

Peer reviewed

HHS Public Access

Author manuscript

ACS Appl Mater Interfaces. Author manuscript; available in PMC 2021 February 05.

Published in final edited form as:

ACS Appl Mater Interfaces. 2020 February 05; 12(5): 6159–6168. doi:10.1021/acsami.9b16193.

An Innovative Nanobody-based-Electrochemical Immunosensor Using Decorated Nylon Nanofibrous for Point-of-Care Monitoring of Human Exposure to Pyrethroid Insecticides

Ahmed Y. El-Moghazy[1,2,*], **Jingqian Huo**[3,4], **Noha Amaly**[1,2], **Natalia Vasylieva**[3], **Bruce D. Hammock**[3], **Gang Sun**[1,*]

[1]Department of Biological and Agricultural Engineering, University of California, Davis, CA 95616, USA.

[2]Polymeric Materials Research Department, Advanced Technology and New Materials Research Institute, City of Scientific Research and Technological Applications (SRTA-City), New Borg El-Arab City 21934, Alexandria, Egypt.

[3]Department of Entomology and Nematology and UCD Comprehensive Cancer Center, University of California, Davis, California 95616, United States.

[4]College of Plant Protection, Agricultural University of Hebei, Baoding 071001, P. R. China.

Abstract

A novel ultrasensitive nanobody-based electrochemical immunoassay was prepared for assessing human exposure to pyrethroid insecticides. 3-Phenoxybenzoic acid (3-PBA) is the common human urinary metabolite for numerous pyrethroids which broadly served as a biomarker for following the human exposure to these pesticides group. The 3-PBA detection was *via* a direct competition for binding to alkaline phosphatase-embedded nanobodies between free 3-PBA and a 3-PBA-bovine serum albumin conjugate covalently immobilized onto citric acid decorated Nylon nanofibers, which were incorporated on a screen-printed electrode (SPE). Electrochemical impedance spectroscopy (EIS) was utilized to support the advantage of the employment of nanofibrous membranes and the success of the immunosensor assembly. The coupling between the nanofiber and nanobody technologies provided an ultra-sensitive and selective immunosensor for 3-PBA detection in a range of 0.8 to 1000 pg mL^{-1}, with a detection limit of 0.64 pg mL^{-1}. Moreover, when the test for 3-PBA was applied to real samples, the established immunosensor proved to be a viable alternative to the conventional methods for 3-PBA detection in human urine even without sample cleanup. It showed excellent properties and stability over time.

Keywords

Nylon; Nanofibers; Electrochemical immunosensor; Nanobody; Pyrethroids; Point-of-care; 3-PBA

* aelmoghazy@ucdavis.edu, gysun@ucdavis.edu.

1. Introduction:

Nanofibers (NFs) and nanofibrous membranes (NFMs) produced *via* electrospinning are promising materials, due to their ultrahigh specific surface areas, and have received a growing interest for their applications in many fields including environmental [1-3], energy [4,5], medical [6-8], food applications [1,9]. One of the aspects on which biosensor performance depends is the sensor matrix material. An appropriate matrix provides high loading capacity for biorecognition elements and accessibility of target analytes to the active sites. As a result, the employment of the nanofibers with the high surface areas and microporous network in the development of the sensors has produced higher sensitivity and lower limits of detection (LOD) to toxicants [9,10]. Polycaprolactam (Nylon 6) fibers, commonly known as polyamide fibers, have been commonly served as media supporting materials owing to their desired chemical stability and biocompatibility as well as notable mechanical properties_[11]. However, compared with other polymers such as polyvinyl alcohol and cellulose, polyamide is lack of reactive groups for chemical modifications and biomolecule immobilization. Polyamide fibers incorporated with desired reactive groups are ideal media for various applications such as protein immobilization[12].

Pyrethroids are widely used synthetic insecticides for agricultural and private household uses, as an alternative to organophosphate insecticides [13,14]. The impacts of exceptionally high pyrethroid exposure include many harmful effects. Moreover, long term exposure to high levels of these synthetic insecticides may contributes developmental neuro-toxicity[15], harmful impacts on male reproduction [16], and endocrine system disruption [17].

3-Phenoxybenzoic acid (3-PBA) is the most known metabolite from hydrolysis of numerous pyrethroids pesticides [18-20]. These pyrethroids in mammals are hydrolyzed by esterases to 3-phenoxybenzyl alcohol or 3-phenoxybenzaldehyde, which rapidly turned into 3-PBA. Hence, 3-PBA is widely employed as the common biomarker for human pyrethroids exposure [19,21], although it has other uses as well.

Using 3-PBA in analysis of pyrethroid metabolite have been reported [22-27], with high sensitivity and accuracy in different real samples. However, they are not convenient and practical for field sensing and monitoring applications and require expensive instruments, highly trained people and transport to central laboratory. Although the tremendous popularity of ELISA, the feasibility of it as a point-of-care monitoring tool is hard to realize.

Electrochemical biosensors are commonly assembled for point-of-care applications owing to their unique merits such as rapid real-time detection and the operational procedures for on-site analysis application. Electrochemical immunosensing systems are receiving an expanding attention) due to the operational simplicity, high sensitivity and high selectivity toward the desired target; depending on the specific antibody-antigen interaction on the electrode surface [28]. Nevertheless, the instability of recombinant antibodies requires a very careful fabrication and application processes.

Nanobodies (Nbs), termed variable heavy chain (VHH) domains or single-domain antigen-binding fragments, are derived from heavy-chain only antibodies that occur naturally in the serum of camelids [29]. Several advantages the Nbs could afford over the traditional

antibodies) such as small size and ease of expression, more thermal and chemical stable, high solubility, suitability for determination of the small molecules (MW< 1500 Da) in the different matrices, proteolysis resistance, and ease of genetic manipulation [30,31], as well as the intact and unique antigen-binding antibody fragments [30]. However, research on use of the Nbs in electrochemical sensors is still limited.

Herein, we adapted and integrated different technologies, including nanofibrous materials, nanobodies, and electrochemical methods to develop a novel sensitive electrochemical competitive immunosensor for rapid assaying of 3-PBA. The nanosensor is assembled based on use of novel Nylon nanofibrous membranes that were surface modified with citric acid (CA) and a nanobody-alkaline phosphatase (Nb-ALP) fusion protein. The proposed immunosensor was fabricated by immobilization of 3-PBA onto the surface of the CA and Nb-ALP decorated Nylon nanofibrous membrane and then incorporation of the membrane onto a screen-printed electrode (SPE). Differential pulse voltammetry (DPV) was used to determine the activity of the alkaline phosphatase.

2. Chemicals, Materials, and Instrument.

Polycaprolactam (Nylon 6, Ny), formaldehyde, formic acid, citric acid (CA), 3-phenoxybenzoic acid, and its analogues, permethrin, cypermethrin, deltamethrin, fenpropathrin, phenothrin, ethanolamine (EA), 1-naphthyl phosphate (1-NP) and *p*-nitrophenyl phosphate (pNPP) were supplied by Sigma (St. Louis, MO) and used as received. N-Ethyl-N′-(3- dimethyl aminopropyl) carbodiimide hydrochloride (EDC), N-hydroxyl succinimide (NHS), disodium hydrogen phosphate (Na_2HPO_4), monosodium orthophosphate (NaH_2PO_4), and O-phosphoric acid (85%) were purchased from Acros Chemical (Pittsburgh, PA, USA). All other chemicals were of analytical grade and were supplied by Merck (Darmstadt, Germany).

A 263A potentiostat/galvanostat equipped with a frequency response detector (FRD100) (Princeton Applied Research Co., Oak Ridge, TN, USA) was used for the electrochemical measurements. The disposable SPE, comprising a carbon working electrode, a carbon counter electrode, and an Ag/AgCl reference electrode, was purchased from eDAQ Inc. (Colorado, US). The morphological characterizations of the polymeric nanofibrous membranes were implemented by a FEI 430 Nova NanoSEM scanning electron microscope (SEM).

The FT-IR spectra of membrane materials were achieved by using a Nicolet 6700 spectrometer, following of the pressing of the grounded the Ny NFMs at the different reaction steps with anhydrous KBr, FT-IR spectra of these specimens were scanned in the wavenumber range of 500-4000 cm^{-1} with a resolution of 4 cm^{-1}.

2.1. Fabrication of Nylon 6 nanofibrous membranes (Ny NFM)

A formic acid solution of Nylon 6 (15% w/v) was prepared with using mechanical stirring at 60 °C for 8 h. Electrospinning was carried out using a 10-mL plastic syringe with an 18-gauge tubular metal needle with a flat tip. The nylon nanofibrous membranes were fabricated through electrospinning of the nylon solution at the room temperature utilizing a

DXES-1 spinning equipment supplied with an applied voltage of 20 kV and spinning rate of 0.7 mL/h with a 23 cm the needle tip far from the collector surface. The resultant Nylon nanofibrous membranes (Ny NFM)_were kept for 12 h in a vacuum oven at 40 °C for drying. The Nylon solution (15% w/v) was used to cast a thin membrane film (Ny-CM) in similar thickness to the Ny NFM. A 4 mm Ny NFM disc with 0.05 mm thickness was laminated on the working electrode of the SPE using a conductive paste to fabricate Ny NFM/SPE, and similarly an Ny CM/SPE was prepared in parallel by using an Ny CM disc.

2.2. Chemical modifications of Nylon nanofibrous membranes

Ny NFMs were chemically modified according to reactions shown in Scheme 1. Firstly, Nylon 6 NFMs were turned to N-methylol Nylon 6 by converting of the amide (N-H) groups to N-methylol groups *via* reacting with formaldehyde and the product was designated as Ny-OH NFMs [32,33]. Briefly, 2 g of Ny NFM were immersed in 25 mL of formaldehyde (36.5% w/v) and 0.2 mL phosphoric acid (85% w/w) at temperature 60 °C for about 1 hour. Then the prepared Ny-OH NFMs were washed several times with distilled water.

The hydroxyl groups on the Ny-OH NFMs were then reacted with the carboxylic groups of citric acid (CA) in a procedure performed as follows [3]: A CA solution 8 % (w/v) was prepared *via* dissolving CA in 10 mL of PBS buffer pH 7.2, synchronously EDC and NHS were added into the CA solution at a final concentration of 1 mM. This blend was energetically mixed at room temperature for 2 hours. Afterwards, the as-prepared Ny-OH NFMs were dipped into the CA/EDC/NHS solution for 60 min at 60 °C. Subsequently, the resulted membranes (Ny-CA NFM) were washed by PBS and dried in a vacuum oven at 80 °C for 1 h.

2.3. Production of Anti-3-PBA Nb–ALP Fusion Protein

The Nb–ALP fusion protein with a 6× His tag at its C-terminal end was created as depicted previously [34]. Briefly, primers were used to amplify the Nb gene (forward primer: GAG GAG GAG GTG GCC CAG CCG GCC CAG GTG CAG CTC GTG GAG TCT GGG GGA, reverse primer: GAG GAG GAG CTG GCC CCC GAG GCC GCG TCT TGT GGT TTT GGT GTC TTG GG). After a ligation reaction, the ligation products were then transformed into chemically competent cells of *E. coli* strain BL21(DE3) pLysS, then the positive clones grown on the plates were picked up for sequencing, and this was followed by multiplication, induction and purification of the crude fusion protein by affinity chromatography using a high-capacity nickel-immobilized-metal-ion-resin column. The elution of the purified Nb-ALP fusion protein was carried out with elution buffer (PBS containing 100 mM imidazole), subsequently by the dialysis with PBS at 4 °C for 72 h to obtain the Nb–ALP fusion protein and stored at −20 °C to use.

2.4. Fabrication of the immunosensor:

Firstly, the carboxylic groups of the Ny-CA NFM/SPE were activated by incubation with 100 μL of 1mM EDC/NHS for 1 hr. After being rinsed with PBS, 6 μL of 3-phenoxybenzoic acid/bovine serum albumin conjugate (3PBA-BSA) prepared according to Shan et. al., (2003) [35] at concentration of 10 μg/mL in PBS were dropped onto the surface of EDC/NHS decorated Ny-CA NFM/SPE for 2 hr at 4 °C. Followed by the washing with PBS to remove

any un-immobilized antigen, the remaining active groups were blocked with 100 μL of 2% ethanolamine (EA) at room temperature for 1 hr, and then rinsed again with PBS and stored at 4°C to use.

The competition step was performed by incubating 50 μL of Nb-ALP (400 μg mL^{-1}) and equivalent volume from different concentrations of 3-PBA on the immunosensor surface for 40 min at room temperature. In the wake of washing multiple times by PBST (PBS containing 0.5% Tween 20), the ALP activity was measured electrochemically using Differential pulse voltammetry (DPV). The assembly steps of the 3-PBA nanosensor and detection mechanism are illustrated in the following schematic diagram (Scheme 2).

2.5. Electrochemical measurements

Electrochemical impedance spectroscopy (EIS) was used for characterizing of the immunosensor surface using ferri/ferrocyanide ($[Fe(CN)_6]^{4-/3-}$) dissolved in PBS at concentration of 2.5 mM. The Nyquist plots were recorded at an applied potential of 0.09 V *vs* Ag/AgCl, with a frequency range from 10 KHz to 1 Hz. DPV measurements were carried out with applied potential range of 0–400 mV, pulse amplitude 60 mV, pulse period 200 ms, pulse width 100 ms and scan rate of 50 mV/s. The signal generation depends on ALP dephosphorylates of non-electroactive 1-NP to 1-naphthol, which electrochemically oxidized to 1-iminoquinone on the electrode surface.

2.6. Applicability of the nanosensor for real sample analysis

Urine samples were gathered from a healthful person and spiked with various concentrations of 3-BPA from 0.01 to 0.5 ng mL^{-1} after the negative 3-PBA content verified using LC-MS. The resulting samples were then diluted 10 times with PBS followed by direct analysis using the assembled nanobody-based-sensor.

3. Results and Discussion

3.1. Morphologies and Structure

The nanosensor was designed based on the use of a chemically modified Nylon nanofibrous membrane as a supporting matrix with immobilized antigen to satisfy the following important principles: (I) the hydrophilicity of the matrix that improves the performance of the sensor in aqueous samples, (II) the physical and chemical characteristics of Nylon as a robust matrix for the fabrication and detection processes, and (III) the ultrahigh surface and microporous areas that can increase the efficiency and the accessibility of the active sites to the targets.

The morphologies of the Nylon NFMs during the different steps of chemical modifications were characterized by scanning electron microscopy (SEM). As shown in Figure 1 (a and b), the Nylon NFMs revealed randomly oriented three-dimensional nonwoven membrane structures with an average fiber diameter of 75 nm. The average diameter of the nanofiber increased to 90 nm after the reaction with formaldehyde in acidic medium (Figure 1(c and d)). Consequently, the nanofiber diameter was further increased to 100-110 nm after incorporation of CA, as illustrated in Figure 1(e and f). The increase of the nanofiber

diameters after the modifications were possibly due to increased hydrophilicity and swelling behavior of the methylolated and carboxylated Nylon fibers, and the impregnations of the fibers with the different aqueous solutions through the modifications [36]. This observation agreed well with the water wetting properties of the Nylon NFMs before and after the modification, where the contact angle measurements (Figure S2) decreased from 85° for the non-modified Nylon NFM to 52° for the CA grafted Ny NFM during a contact time of 30 sec, attributing to the presence of hydroxyl and carboxyl groups after the modifications by formaldehyde and citric acid, respectively.

FT-IR spectroscopy was utilized to characterize successful grafting of CA onto the NFM. FTIR spectra of the pristine Nylon nanofibers before and after modifications are shown in Figure 2. The conversion of the amide groups of Nylon to hydroxyl groups by formaldehyde was confirmed by the appearance of a new peak at 1042 cm^{-1} for the C-O of primary alcohol, broadening band in the region 3250–3500 cm^{-1}, corresponding to the stretching mode of formed hydroxyl groups on the surface of the Nylon NFM. Also, a relatively weak decrease in the intensity of C=O, N-H of amide peaks at 1630 cm^{-1} and 1552 cm^{-1}, respectively, can be the evidence of the reaction on N-H group in the Nylon.

The appeared peak of C=O of the ester at 1750 cm confirmed the effective incorporation of carboxyl groups onto the Nylon NFM surface between the methylene hydroxy (CH_2OH) on the Nylon and carboxylic acid (-COOH) group of CA [3,37], and the decrease of hydroxyl group peak intensity at 1042 cm^{-1}. With increase of the initial CA concentration, the intensity of the new peak at 1750 cm^{-1} of the resulting ester was increased correspondingly. The same trend in intensity change was observed at 1040 cm^{-1} (Figure S1).

3.2. Electrochemical characterization

EIS is a suitable tool for studying the surface features of the different modified electrode through the assembling and the dynamic performances of electrochemical processes [38]. Herein, the EIS was used to study the advantages of the nanofibrous membranes and to validate the sensors fabricated through these steps. The most common equivalent circuit which used in the electrochemical immunosensors development provided by Randles [39-41]. As shown in Figure 3A (inset), the components of the circuit are the electrolyte resistance (R_s), the electron-transfer resistance (R_{et}), capacitance of the double-layer (C_d) and Warburg impedance (Z_w), where R_s and Z_w represent the resistance of the supporting electrolyte and the diffusion properties of the redox probe in the solution, respectively, and are not affected by the occurred modifications on the electrode surface. The Nyquist plot contains two parts. At the higher frequencies, a semicircle portion reflects R_{et} of the surface of the electrode, which is the most important parameter, and its value changed due to the modification and interaction of the electrode surface with the electrolyte. The second part at the lower frequencies is a linear portion which presents the diffusion-limited process [42]. As shown in Figure 3A, the Nyquist plot of the bare SPE reveals a very low resistance value (curve a). The modification of SPE with the casted Nylon membrane (Ny-CM) exhibited a dramatic increase in the resistance of the electron transfer due to the insulation of the electrode surface by the Ny-CM (curve b). While with the replacement of the casted membrane by the nanofibrous membrane (Ny NFM) with its distinctive porous structure decreased the R_{et} by

more than 5 times (curve c), facilitates the access of $[Fe(CN)_6]^{4-/3-}$ and accelerates the electron transfer toward the electrode surface, making this unique material introduced as an ideal matrix for fabricating highly sensitive sensing systems.

The fabrication of the nanosensor was finalized by the application of the chemically modified nanofibers (Ny-CA) with EDC/NHS as a supported matrix for immobilization of 3PBA-BSA. Figure 3B confirmed the success of the fabrication steps. The bare SPE showed very low electron-transfer resistance (curve a). After the lamination of the electrode surface with the Nylon nanofibrous, the semicircle increased, revealing that the nanofibrous membranes acted as an electron transfer barrier (curve b). The grafting of CA onto the Ny NFM enhanced the hydrophilicity (Figure S2) but induced a small increase of the R_{et} (curve c), which could be ascribed to the electrostatic repulsion between the same negative charge of $[Fe(CN)_6]^{3-/4-}$ and carboxylic groups of the CA. The activation of the modified Nylon nanofibrous with EDC/NHS induced decrease of R_{et} (curve d), possibly owing to the replacement of the carboxyl group by NHS groups, that facilitates the electrolyte move through the porous structure of the nanofibrous membranes. The deterred electron transfer continued with immobilization of 3PBA-BSA, blocking of the unreacted sites and reaction with Nb-ALP (curve e, f and g), evidence of the effective immobilization of blocking groups. All the EIS results confirmed the successful assembly of the nanosensor.

3.3. Experimental parameters optimization

In order to accomplish the most effective analytical performance of the fabricated immunosensor for 3-PBA detection, different important experimental conditions were optimized by measuring the achieved currents using DPV, which include 3PBA-BSA concentration, requierd time for immobilization of 3PBA-BSA, Nb-ALP concentration, the immunoreaction time, substrate concentration, and the blocking process.

3.3.1. Antigen concentration: The 3PBA-BSA concentration was optimized using the reaction with the Ny-CA NFM/SPE, an incubation time of 2hr, Nb-ALP concentration of 400 μg mL^{-1}, substrate concentration of 1mg mL^{-1}, and immunoreaction time of 40 min. As shown in Figure 4 (a), the current response increased gradually with the increment of the 3PBA-BSA concentration and the maximum response at a concentration of 10 μg mL^{-1} was observed. Nevertheless, the higher concentrations than 10 μg mL^{-1} prompted a decline in the current achieved. This may be due to the steric hindrance of membrane that could obstruct the ability of nanobodies to reach the binding sites on the nanofibers surfaces and the moving of the electrons from the analyte solution toward the electrode surface.

3.3.2. Antigen immobilization time: The necessary time for the 3PBA-BSA immobilization on the Ny-CA NFM/SPE was adjusted at 3PBA-BSA concentration of 10 μg mL^{-1}, Nb-ALP concentration of 400 μg mL^{-1}, substrate concentration of 1mg mL^{-1} and immunoreaction time of 40 min. As seen in Figure 4 (b), expanding of the immobilization time of the Ny-CA NFM/SPE with 3PBA-BSA from 30 min up to 120 min resulted in an increase of the current response and achieved a plateau at the incubation time over 120 min, revealing the saturation of the immobilization sites of the nanofibrous membrane. 120 min was selected as a tethering time for the further experiments.

3.3.3. Nanobody concentration: The nanobody concentration is considered as a key factor in the development of the sensitive competitive immunoassays as the increase of the nanobody concentration decreases the sensitivity of the immunosensor, and lower nanobody concentrations reduce the signal response. For the optimization of the nanobody concentration, the fabricated immunosensor immobilized with 10 μg mL^{-1} 3PBA-BSA for 120 min was incubated with different Nb-ALP concentrations in a range of 100 to 600 μg mL^{-1} for 40 min. The current responses were recorded at a substrate concentration of 1mg mL^{-1}. As observed in Figure 4 (c), the signal response was directly proportional to the Nb-ALP concentration, and until a concentration of 400 μg mL^{-1} the increase in the generated current was achieved, which was selected for the electrochemical assays.

3.3.4. Immunoreaction time: The optimization of the immunoreaction time was carried out by incubating the fabricated immunosensor (3PBA-BSA concentration of 10 μg mL^{-1}, immobilization time of 120 min and substrate concentration of 1mg mL^{-1}) with Nb-ALP at a concentration of 400 μg mL^{-1} for different times. The signal response gradually increased with the increasing time to reach a maximum and then to a platform at the time of 40 min (Figure 4 (d)), indicating that there was no available free nanobody to match with the immobilized 3PBA-BSA after that time.

3.3.5. The substrate concentration: Finally, the concentration of the substrate is another critical factor affecting the enzyme-catalyzed reaction[26]. With the other parameters fixed, the current response increased continuously with the concentration of 1-NP and reached the maximum value at the concentration of 1mg mL^{-1} (Figure 4 (e)). No further obvious increase in the response with an increase of the substrate concentration was observed afterward. So, 1 mg mL^{-1} was adopted as the ideal concentration for the best analytical performance.

3.3.6. Blocking of remaining active sites of NFM: It is necessary to block any residual free active groups on the chemically modified and coating antigen incorporated nanofiber surface to prevent any non-specific reaction with Nb-ALP during the competition step. Incomplete blockage of the sites could affect the accuracy of the immunosensor. In some cases, the type and concentration of blocking reagents can have a large effect on assay performance. Two blocking reagents, bovine serum albumin (BSA) and ethanolamine (EA), in concentration of 2% (w/v) were assayed. Samples of 5 mm of Ny-CA NFM and Ny-CA CM discs were incubated with the blocking solutions for 12 hr at 4°C, respectively. After washing with PBS, 100 μl of Nb-ALP at concentration of 400 μg mL^{-1} were added onto the discs for 2 hr in the room temperature. Consequently, the discs were washed several times with a Vortex® mixer in PBS to remove unbonded Nb-ALP. The efficiency of the blocking process was evaluated colorimetry based on the colorimetric analysis of the ALP enzyme activity using *p*-nitrophenyl phosphate (*p*NPP) substrate. The control samples were incubated with no blocking solutions (only PBS). As shown in Figure 4 (F), in the case of the activated CA-Ny CM, both reagent solutions showed the ability for fully blocking of the active groups on the surface of the membranes. On the other hand, the use of BSA resulted in insufficient blocking for the active groups on the surface of the activated CA-Ny NFM, while EA observed totally blockage of the active sites of the nanofibrous membranes. The

microporosity of the nanofibrous membranes might have restricted BSA from penetrating into the membranes since the BSA molecular size (66.5 kDa) is quite large, almost 4 times larger than the nanobody molecular size (about 15 kDa) [43,44].

3.4. Detection of 3-phenoxybenzoic acid

With optimizing the different factors, the analytical performance of the fabricated nanosensor for 3-PBA detection was investigated based on a competition between the free and immobilized 3-PBA to bind with the nanobody in the solution, followed by measuring ALP-impeded-Nb activity electrochemically using 1-NP substrate. Figure 5A shows the DPV responses of the assembled nanosensor at different 3-PBA concentrations, it was obvious that the current achieved decreased as 3-PBA concentration increased. As illustrated in Figure 5B, the current responses exhibited a linear decrease with the logarithm of 3-PBA concentration from 0.0008 to 1 ng mL^{-1} and could be fitted into a linear regression equation: I% = 12.925 log c/ng mL^{-1} + 93.235 (R^2=0.9913). The developed immunosensor demonstrated a high sensitivity toward 3-PBA with a limit of detection (LOD) at 0.64 pg mL^{-1} (LOD=3Sb /m, where Sb is the standard deviation of the blank and m is the slope of the calibration plot.). When compared the assembled electrochemical immunosensor to other 3-PBA detection methods (Table 1), the assembled nanobody-based-sensor observed a good behavior in term of LOD, the ultra-high sensitivity of the nanosensor could be attributed to the integration of the different technologies, including the microporous nanofibrous membranes enhancing the accessibility of the nanobody to the recognition sites and accelerating the electron transfer consequently improving the sensing surface and the utilization of the nanobodies with their merits as an alternative to the traditional antibodies, allowing detection of the 3-PBA with high sensitivity.

3.5. Specificity, reusability, and stability of the immunosensor

The ability of a sensor to specifically detect the desired target in samples containing different analogs and other molecules is considered as one of the most important challenges in the sensing technology field. The selectivity of the assembled immunosensor was investigated by examining 0.1 ng mL^{-1} of two 3-PBA analogues (3-phenoxybeneyl aldehyde and 3-phenoxybenzyl alcohol) and three pyrethroids (permethrin, cypermethrin and deltamethrin) pesticides. The cross-reactivity (CR %) was studied by determining the residual current response after the competitions between each molecule and immobilized 3PBA-BSA to bind with the nanobodies. It was in terms of 3-PBA-equivalent concentration and expressed as a percentage of 3-PBA response [9,50]. As seen in Table 2, the assembled nanosensor presented a very high specificity to 3-PBA. Whereas, the different tested material did not exbibit cross-reactivity, except 3-phenoxybeneyl aldehyde, which showed a low cross-reactivity (12.9%). This compound can rapidly convert to 3-PBA in the human body [51].

The reusability of the sensors could be useful for minimizing the cost of the medical screening tests and reducing medical wastes. The assembled immunosensor was regenerated by dipping in 0.1M of glycine hydrochloric acid buffer at pH value of 2.8 for 5 min after detection of o.1 ng mL^{-1} of 3-PBA. The assembled immunosensor demonstrated good reusability by maintaining more than 90% of its initial activity in the second cycle and about

66% after 3 assay runs (Figure S3). The activity loss may be due to denaturation of the bovine serum albumin or destruction of Ny NFM with repeating the regeneration in an acidic glycine buffer [52].

The immunosensor was stored at 4°C and its activity was evaluated every week to study the stability. The immunosensor showed good stability by maintaining more than 90% of its original activity after 5 weeks.

3.6. Applicability of the immunosensor

In order to investigate practicality and feasibility of the assembled nanosensor in detection of trace amounts of 3-BPA in real samples, human urine samples were spiked with known concentrations of 3-BPA ranging from 0.01 to 0.5 ng mL^{-1}. Preceding the spiking process, the urine samples were verified by LC-MS to be free of 3-BPA. The spiked urine samples were diluted 10 times with PBS without any further treatments then were analyzed by the immunosensor in a blind fashion. Each concentration was tested in triplicate. As illustrated in Table S1, the recovery rate was from 94.8% to about 102% and the relative standard deviation (RSD%) was about 4.7%. The above-mentioned results prove the applicability, accuracy and reproducibility of the assembled nanosensor for fast 3-PBA detection in the human urine at extremely lower concentration without pre-cleaning for the samples.

4. Conclusion

An ultrasensitive, disposable, and rapid detection immunosensor for monitoring human exposure to pyrethroid pesticides was successfully developed by coupling a nanobody Nb-ALP to surfaces of the nanofibers in microporous nanofibrous membranes. The developed nanosensor exhibited very attractive analytical performance with a competitive detection limit of 0.64 pg mL^{-1}. The fabricated immunosensors possess the advantage of easy use, low-cost assay, reusability, and fast analysis, where the sample analysis could be accomplished in less than 45 min. The new immunosensor could be a promising alternative tool to the traditional methods for point-of-care detection of 3-PBA.

Supplementary Material

Refer to Web version on PubMed Central for supplementary material.

Acknowledgement

The National Institute of Environmental Health Science Superfund Research Program (P42ES004699) and the National Academy of Sciences (NAS, Subaward No. 2000009144). *The article is derived from the Subject Data funded in part by NAS and USAID, and that any opinions, findings, conclusions, or recommendations expressed in such article are those of the authors alone, and do not necessarily reflect the views of USAID or NAS*. The National Nature Science Foundation of China (No. 31471786).

References:

(1). Hu M-X; Li J-N; Guo Q; Zhu Y-Q; Niu H-M Probiotics Biofilm-Integrated Electrospun Nanofiber Membranes: A New Starter Culture for Fermented Milk Production. J. Agric. Food Chem 2019, 67 (11), 3198–3208. 10.1021/acs.jafc.8b05024. [PubMed: 30838858]

(2). Li X; Wang C; Huang X; Zhang T; Wang X; Min M; Wang L; Huang H; Hsiao BS Anionic Surfactant-Triggered Steiner Geometrical Poly(Vinylidene Fluoride) Nanofiber/Nanonet Air Filter for Efficient Particulate Matter Removal. ACS Appl. Mater. Interfaces 2018, 10 (49), 42891–42904. 10.1021/acsami.8b16564. [PubMed: 30427661]

(3). Amaly N; Si Y; Chen Y; El-Moghazy AY; Zhao C; Zhang R; Sun G Reusable Anionic Sulfonate Functionalized Nanofibrous Membranes for Cellulase Enzyme Adsorption and Separation. Colloids Surfaces B Biointerfaces 2018, 170, 588–595. 10.1016/J.COLSURFB.2018.06.019. [PubMed: 29975907]

(4). Ramadan M; Abdellah AM; Mohamed SG; Allam NK 3D Interconnected Binder-Free Electrospun MnO@C Nanofibers for Supercapacitor Devices. Sci. Rep 2018, 8 (1), 7988 10.1038/s41598-018-26370-z. [PubMed: 29789633]

(5). Liu X; Naylor Marlow M; Cooper SJ; Song B; Chen X; Brandon NP; Wu B Flexible All-Fiber Electrospun Supercapacitor. J. Power Sources 2018, 384, 264–269. 10.1016/J.JPOWSOUR.2018.02.081.

(6). Awada H; Al Samad A; Laurencin D; Gilbert R; Dumail X; El Jundi A; Bethry A; Pomrenke R; Johnson C; Lemaire L; et al. Controlled Anchoring of Iron Oxide Nanoparticles on Polymeric Nanofibers: Easy Access to Core@Shell Organic-Inorganic Nanocomposites for Magneto-Scaffolds. ACS Appl. Mater. Interfaces 2019, 11 (9), 9519–9529. 10.1021/acsami.8b19099. [PubMed: 30729776]

(7). Mao Z; Li J; Huang W; Jiang H; Zimba BL; Chen L; Wan J; Wu Q Preparation of Poly(Lactic Acid)/Graphene Oxide Nanofiber Membranes with Different Structures by Electrospinning for Drug Delivery. RSC Adv. 2018, 8 (30), 16619–16625. 10.1039/C8RA01565A.

(8). Wang Y; Cui W; Zhao X; Wen S; Sun Y; Han J; Zhang H Bone Remodeling-Inspired Dual Delivery Electrospun Nanofibers for Promoting Bone Regeneration. Nanoscale 2019, 11 (1), 60–71. 10.1039/C8NR07329E.

(9). El-Moghazy AY; Zhao C; Istamboulie G; Amaly N; Si Y; Noguer T; Sun G Ultrasensitive Label-Free Electrochemical Immunosensor Based on PVA-Co-PE Nanofibrous Membrane for the Detection of Chloramphenicol Residues in Milk. Biosens. Bioelectron 2018, 117 (May), 838–844. 10.1016/j.bios.2018.07.025. [PubMed: 30096738]

(10). El-Moghazy AY; Soliman EA; Ibrahim HZ; Marty JL; Istamboulie G; Noguer T Biosensor Based on Electrospun Blended Chitosan-Poly (Vinyl Alcohol) Nanofibrous Enzymatically Sensitized Membranes for Pirimiphos-Methyl Detection in Olive Oil. Talanta 2016, 155, 258–264. 10.1016/j.talanta.2016.04.018. [PubMed: 27216682]

(11). Dong C; Wang H; Zhang Z; Zhang T; Liu B Carboxybetaine Methacrylate Oligomer Modified Nylon for Circulating Tumor Cells Capture. J. Colloid Interface Sci. 2014, 432, 135–143. 10.1016/j.jcis.2014.07.003. [PubMed: 25086387]

(12). Edmondson S, Osborne VL, Polymer WTSH Brushes via Surface-Initiated Polymerizations. Chem. Soc. Rev 2004, 33, 14–18. [PubMed: 14737505]

(13). McCoy MR; Yang Z; Fu X; Ahn KC; Gee SJ; Bom DC; Zhong P; Chang D; Hammock BD Monitoring of Total Type II Pyrethroid Pesticides in Citrus Oils and Water by Converting to a Common Product 3-Phenoxybenzoic Acid. J. Agric. Food Chem 2012, 60 (20), 5065–5070. 10.1021/jf2051653. [PubMed: 22486225]

(14). Casida JE; Quistad GB Golden Age of Insecticide Research: Past, Present, or Future? Annu. Rev. Entomol 1998, 43 (1), 1–16. 10.1146/annurev.ento.43.1.1. [PubMed: 9444749]

(15). Shafer TJ; Meyer DA; Crofton KM Developmental Neurotoxicity of Pyrethroid Insecticides: Critical Review and Future Research Needs. Environ. Health Perspect 2005, 113 (2), 123–136. 10.1289/ehp.7254. [PubMed: 15687048]

(16). Yuan C; Wang C; Gao S-Q; Kong T-T; Chen L; Li X-F; Song L; Wang Y-B Effects of Permethrin, Cypermethrin and 3-Phenoxybenzoic Acid on Rat Sperm Motility in Vitro Evaluated with Computer-Assisted Sperm Analysis. Toxicol. Vitr 2010, 24 (2), 382–386. 10.1016/j.tiv.2009.11.001.

(17). Sun H; Chen W; Xu X; Ding Z; Chen X; Wang X Pyrethroid and Their Metabolite, 3-Phenoxybenzoic Acid Showed Similar (Anti)Estrogenic Activity in Human and Rat Estrogen Receptor α-Mediated Reporter Gene Assays. Environ. Toxicol. Pharmacol 2014, 37 (1), 371–377. 10.1016/j.etap.2013.11.031. [PubMed: 24388911]

(18). Jin-Ok C; Jitsunari F; Asakawa F; Suna S; Manabe Y; Takeda N Study on Biological Monitoring of Fenpropathrin Exposure in Application by Utilizing Urinary 3-Phenoxybenzoic Acid Level. Environ. Health Prev. Med 1998, 2 (4), 145–150. 10.1007/BF02931692. [PubMed: 21432532]

(19). Fortes C; Mastroeni S; Pilla MA; Antonelli G; Lunghini L; Aprea C The Relation between Dietary Habits and Urinary Levels of 3-Phenoxybenzoic Acid, a Pyrethroid Metabolite. Food Chem. Toxicol 2013, 52, 91–96. 10.1016/j.fct.2012.10.035. [PubMed: 23146693]

(20). Trunnelle KJ; Bennett DH; Ahn KC; Schenker MB; Tancredi DJ; Gee SJ; Stoecklin-Marois MT; Hammock BD Concentrations of the Urinary Pyrethroid Metabolite 3-Phenoxybenzoic Acid in Farm Worker Families in the MICASA Study. Environ. Res 2014, 131, 153–159. 10.1016/j.envres.2014.03.003. [PubMed: 24721133]

(21). Liu F; Chi Y; Wu S; Jia D; Yao K Simultaneous Degradation of Cypermethrin and Its Metabolite, 3-Phenoxybenzoic Acid, by the Cooperation of *Bacillus Licheniformis* B-1 and *Sphingomonas* Sp. SC-1. J. Agric. Food Chem 2014, 62 (33), 8256–8262. 10.1021/jf502835n. [PubMed: 25068244]

(22). Chung SWC; Lam CH Development and Validation of a Method for Determination of Residues of 15 Pyrethroids and Two Metabolites of Dithiocarbamates in Foods by Ultra-Performance Liquid Chromatography–Tandem Mass Spectrometry. Anal. Bioanal. Chem 2012, 403 (3), 885–896. 10.1007/s00216-012-5882-1. [PubMed: 22395452]

(23). Ding Y; White CA; Muralidhara S; Bruckner JV; Bartlett MG Determination of Deltamethrin and Its Metabolite 3-Phenoxybenzoic Acid in Male Rat Plasma by High-Performance Liquid Chromatography. J. Chromatogr. B 2004, 810 (2), 221–227. 10.1016/J.JCHROMB.2004.07.033.

(24). Mudiam MKR; Jain R; Singh A; Khan HA; Parmar D Development of Ultrasound-Assisted Dispersive Liquid–Liquid Microextraction–Large Volume Injection–Gas Chromatography–Tandem Mass Spectrometry Method for Determination of Pyrethroid Metabolites in Brain of Cypermethrin-Treated Rats. Forensic Toxicol. 2014, 32 (1), 19–29. 10.1007/s11419-013-0196-3.

(25). Pandey V; Chauhan A; Pandey G; Krishna M; Mudiam R Optical Sensing of 3-Phenoxybenzoic Acid as a Pyrethroid Pesticides Exposure Marker by Surface Imprinting Polymer Capped on Manganese-Doped Zinc Sulfide Quantum Dots. Anal. Chem. Res 2015, 5, 21–27. 10.1016/j.ancr.2015.06.002.

(26). Thiphom S; Prapamontol T; Chantara S; Mangklabruks A; Suphavilai C; Chang Ahn K; Gee SJ; Hammock BD Determination of the Pyrethroid Insecticide Metabolite 3-PBA in Plasma and Urine Samples from Farmer and Consumer Groups in Northern Thailand HHS Public Access. J Env. Sci Heal. B 2014, 49 (1), 15–22. 10.1080/03601234.2013.836862.

(27). Liu Y; Wu A; Hu J; Lin M; Wen M; Zhang X; Xu C; Hu X; Zhong J; Jiao L; et al. Detection of 3-Phenoxybenzoic Acid in River Water with a Colloidal Gold-Based Lateral Flow Immunoassay. Anal. Biochem 2015, 483, 7–11. 10.1016/J.AB.2015.04.022. [PubMed: 25957127]

(28). Felix FS; Angnes L Electrochemical Immunosensors – A Powerful Tool for Analytical Applications. Biosens. Bioelectron 2018, 102, 470–478. 10.1016/J.BIOS.2017.11.029. [PubMed: 29182930]

(29). Rasmussen SGF; Choi HJ; Fung JJ; Pardon E; Casarosa P; Chae PS; Devree BT; Rosenbaum DM; Thian FS; Kobilka TS; et al. Structure of a Nanobody-Stabilized Active State of the B2 Adrenoceptor. Nature 2011, 469 (7329), 175–181. 10.1038/nature09648. [PubMed: 21228869]

(30). Muyldermans S Nanobodies: Natural Single-Domain Antibodies. Annu. Rev. Biochem 2013, 82 (1), 775–797. 10.1146/annurev-biochem-063011-092449. [PubMed: 23495938]

(31). Leduc C; Si S; Gautier J; Soto-Ribeiro M; Wehrle-Haller B; Gautreau A; Giannone G; Cognet L; Lounis B A Highly Specific Gold Nanoprobe for Live-Cell Single-Molecule Imaging. Nano Lett. 2013, 13 (4), 1489–1494. 10.1021/nl304561g. [PubMed: 23458263]

(32). Cairns TL, Foster HD, Larchar AW, Schneider AK, AndSchreiber RS Preparation and Properties of N-Methylol, N-Alkoxym Ethyl and N-Alkylthiomethyl Polyamides. J. Am. Chem. Soc 1949, 71, 651–660.

(33). Shieh J-J; Huang RYM Preparation of N-Methylol Nylon-6 Membranes for Pervaporation of Ethanol-Water Mixtures. J. Appl. Polym. Sci 1997, 64 (5), 855–863. 10.1002/(SICI)1097-4628(19970502)64:5<855::AID-APP5>3.0.CO;2-O.

(34). Huo J; Li Z; Wan D; Li D; Qi M; Barnych B; Vasylieva N; Zhang J; Hammock BD Development of a Highly Sensitive Direct Competitive Fluorescence Enzyme Immunoassay Based on a Nanobody–Alkaline Phosphatase Fusion Protein for Detection of 3-Phenoxybenzoic Acid in Urine. J. Agric. Food Chem 2018, 66, 11284–11290. 10.1021/acs.jafc.8b04521. [PubMed: 30293433]

(35). Shan G; Huang H; Stoutamire DW; Gee SJ; Leng G; Hammock BD A Sensitive Class Specific Immunoassay for the Detection of Pyrethroid Metabolites in Human Urine. Chem. Res. Toxicol 2004, 17 (2), 218–225. 10.1021/tx034220c. [PubMed: 14967009]

(36). Fu Q; Wang X; Si Y; Liu L; Yu J; Ding B Scalable Fabrication of Electrospun Nanofibrous Membranes Functionalized with Citric Acid for High-Performance Protein Adsorption. ACS Appl. Mater. Interfaces 2016, 8 (18), 11819–11829. 10.1021/acsami.6b03107. [PubMed: 27111287]

(37). Cerroni B; Cicconi R; Oddo L; Scimeca M; Bonfiglio R; Bernardini R; Palmieri G; Domenici F; Bonanno E; Mattei M; et al. In Vivo Biological Fate of Poly(Vinylalcohol) Microbubbles in Mice. Heliyon 2018, 4 (9), e00770 10.1016/j.heliyon.2018.e00770. [PubMed: 30238062]

(38). Eckhard K; Shin H; Mizaikoff B; Schuhmann W; Kranz C Alternating Current (AC) Impedance Imaging with Combined Atomic Force Scanning Electrochemical Microscopy (AFM-SECM). Electrochem. commun 2007, 9 (6), 1311–1315. 10.1016/J.ELECOM.2007.01.027.

(39). Liu X; Li Q; Chen L; Zhou J; Liu M; Shen Y One-Step Immobilization Antibodies Using Ferrocene-Containing Thiol Aromatic Aldehyde for the Fabrication of a Label-Free Electrochemical Immunosensor. RSC Adv. 2016, 6 (115), 114019–114023. 10.1039/C6RA24122K.

(40). Hammond JL; Formisano N; Estrela P; Carrara S; Tkac J Electrochemical Biosensors and Nanobiosensors. Essays Biochem. 2016, 60, 69–80. 10.1042/EBC20150008. [PubMed: 27365037]

(41). Li Y; Afrasiabi R; Fathi F; Wang N; Xiang C; Love R; She Z; Kraatz H-B Impedance Based Detection of Pathogenic E. Coli O157:H7 Using a Ferrocene-Antimicrobial Peptide Modified Biosensor. Biosens. Bioelectron 2014, 58, 193–199. 10.1016/j.bios.2014.02.045. [PubMed: 24637168]

(42). Santaclara FJ; Pérez-Martín RI; Sotelo CG Developed of a Method for the Genetic Identification of Ling Species (Genypterus Spp.) in Seafood Products by FINS Methodology. Food Chem. 2014, 143, 22–26. 10.1016/j.foodchem.2013.06.004. [PubMed: 24054207]

(43). Wang J; Mukhtar H; Ma L; Pang Q; Wang X VHH Antibodies: Reagents for Mycotoxin Detection in Food Products. Sensors 2018, 18 (2), 485 10.3390/s18020485.

(44). Ren X; Yan J; Wu D; Wei Q; Wan Y Nanobody-Based Apolipoprotein e Immunosensor for Point-of-Care Testing. ACS Sensors 2017, 2 (9), 1267–1271. 10.1021/acssensors.7b00495. [PubMed: 28884572]

(45). Pandey V; Chauhan A; Pandey G; Mudiam MKR Optical Sensing of 3-Phenoxybenzoic Acid as a Pyrethroid Pesticides Exposure Marker by Surface Imprinting Polymer Capped on Manganese-Doped Zinc Sulfide Quantum Dots. Anal. Chem. Res 2015, 5, 21–27. 10.1016/J.ANCR.2015.06.002.

(46). Liu Y; Wu A; Hu J; Lin M; Wen M; Zhang X; Xu C; Hu X; Zhong J; Jiao L; et al. Detection of 3-Phenoxybenzoic Acid in River Water with a Colloidal Gold-Based Lateral Flow Immunoassay. Anal. Biochem 2015, 483 (1), 7–11. 10.1016/j.ab.2015.04.022. [PubMed: 25957127]

(47). Li J; Lin D; Ji R; Yao K; Deng WQ; Yuan H; Wu Q; Jia Q; Luo P; Zhou K; et al. Simultaneous Determination of β-Cypermethrin and Its Metabolite 3-Phenoxybenzoic Acid in Microbial Degradation Systems by HPLC-UV. J. Chromatogr. Sci 2016, 54 (9), 1584–1592. 10.1093/chromsci/bmw108. [PubMed: 27390099]

(48). Pali M; Suni II Impedance Detection of 3-Phenoxybenzoic Acid Comparing Wholes Antibodies and Antibody Fragments for Biomolecular Recognition. Electroanalysis 2018, 30 (12), 2899–2907. 10.1002/elan.201800495.

(49). Pali M; Bever CRS; Vasylieva N; Hammock BD; Suni II Impedance Detection of 3-Phenoxybenzoic Acid with a Noncompetitive Two-Site Phage Anti-Immunocomplex Assay. Electroanalysis 2018, 30, 1–8. 10.1002/elan.201800457.

(50). Gaudin V; Maris P Development of a Biosensor- Based Immunoassay for Screening of Chloramphenicol Residues in Milk. Food Agric. Immunol 2010, No. 2 2015, 37–41. 10.1080/09540100120055648.

(51). Kim Hee-Joo, Ahn Ki Chang, González-Techera Andrés, González-Sapienza Gualberto G., Gee Shirley J., and H BD. Magnetic Bead-Based Phage Anti-Immunocomplex Assay (PHAIA) for the Detection of the Urinary Biomarker 3-Phenoxybenzoic Acid to Assess Human Exposure to Pyrethroid Insecticides. Anal Biochem. 2010, 386 (1), 45–52. 10.1016/j.ab.2008.12.003.Magnetic.

(52). Qiao L; Wang X; Sun X A Novel Label-Free Amperometric Immunosensor Based on Graphene Sheets-Methylene Blue Nanocomposite/Gold Nanoparticles. Int. J. Electrochem. Sci 2014, 9 (3), 1399–1414.

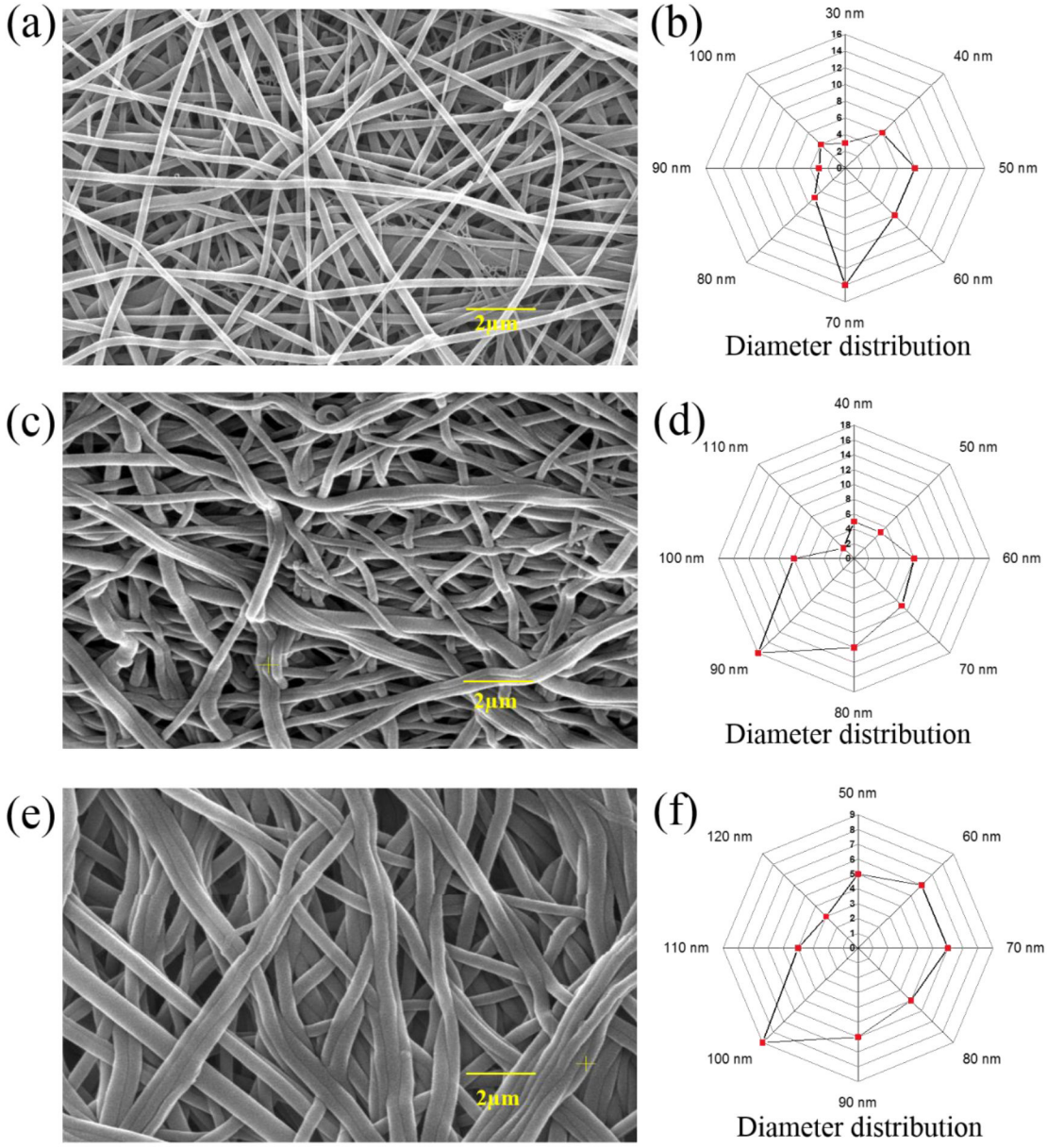

Figure 1:

SEM images of (a) pristine Nylon NFM, (c) Ny-OH NFM, and (e) Ny-CA. Fiber diameter distributions of (b) Nylon NFM, (d) Ny-OH NFM, and (f) Ny-CA.

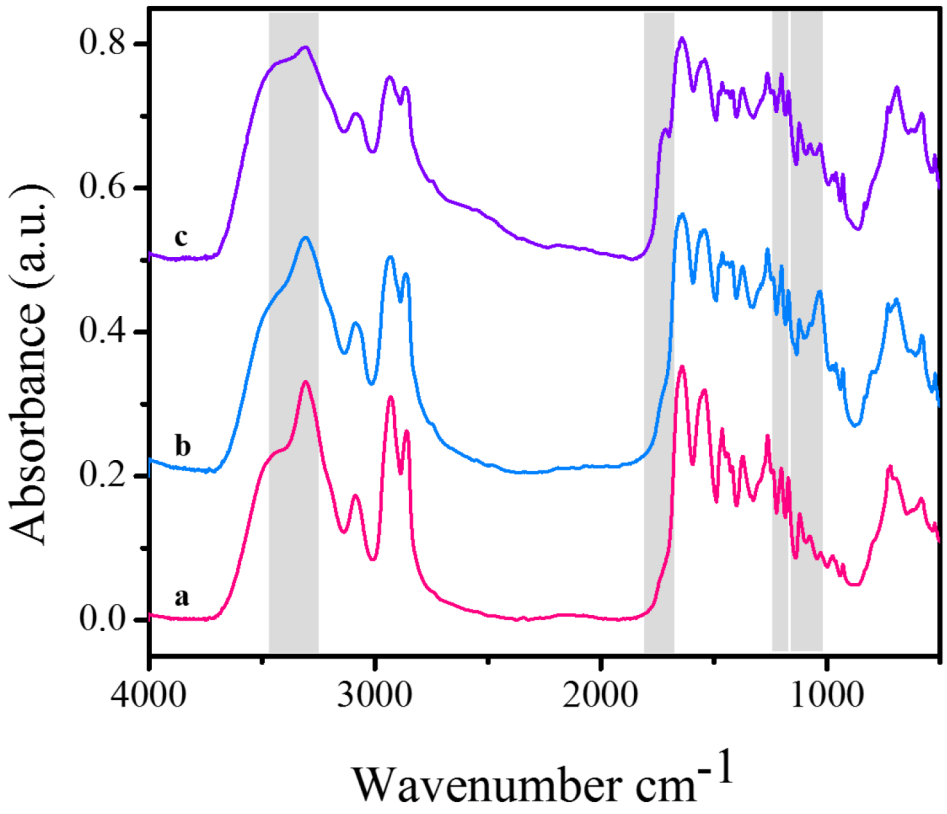

Figure 2:
FT-IR spectra of (a) pristine Ny NFM, (b) N-methylol Ny NFM and (c) Ny NFM grafted with citric acid.

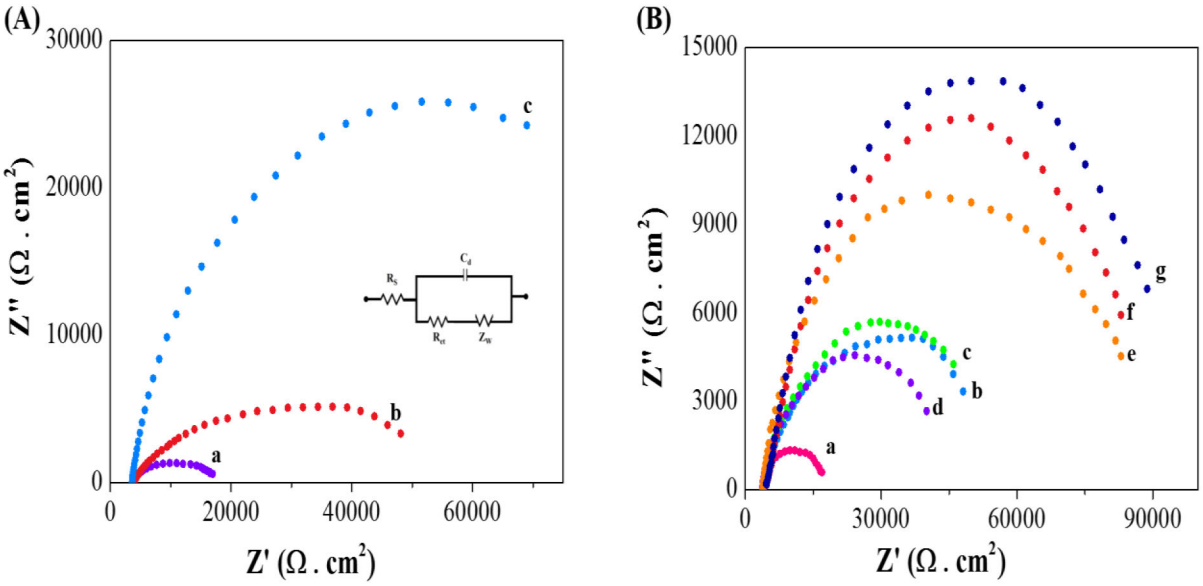

Figure 3:

Electrochemical impedance spectroscopies in 2.5 mM $[Fe(CN)_6]^{4-/3-}$ for: **(A)** bare SPE (a), Ny NFM/SPE (b), and Ny CM/SPE(c); (*Inset: The Randles model for the common equivalent circuit*). **(B)** Assembling steps of the 3-PBA immunosensor: bare SPE (a), Ny NFM/SPE (b), Ny-CA NFM/SPE (c), activated Ny-CA NFM/SPE (d), 3PBA-BSA/ Ny-CA NFM/SPE (e), EA/3PBA-BSA/ Ny-CA NFM/SPE (f) and Nb-ALP/ EA/3PBA-BSA/ Ny-CA NFM/SPE (g).

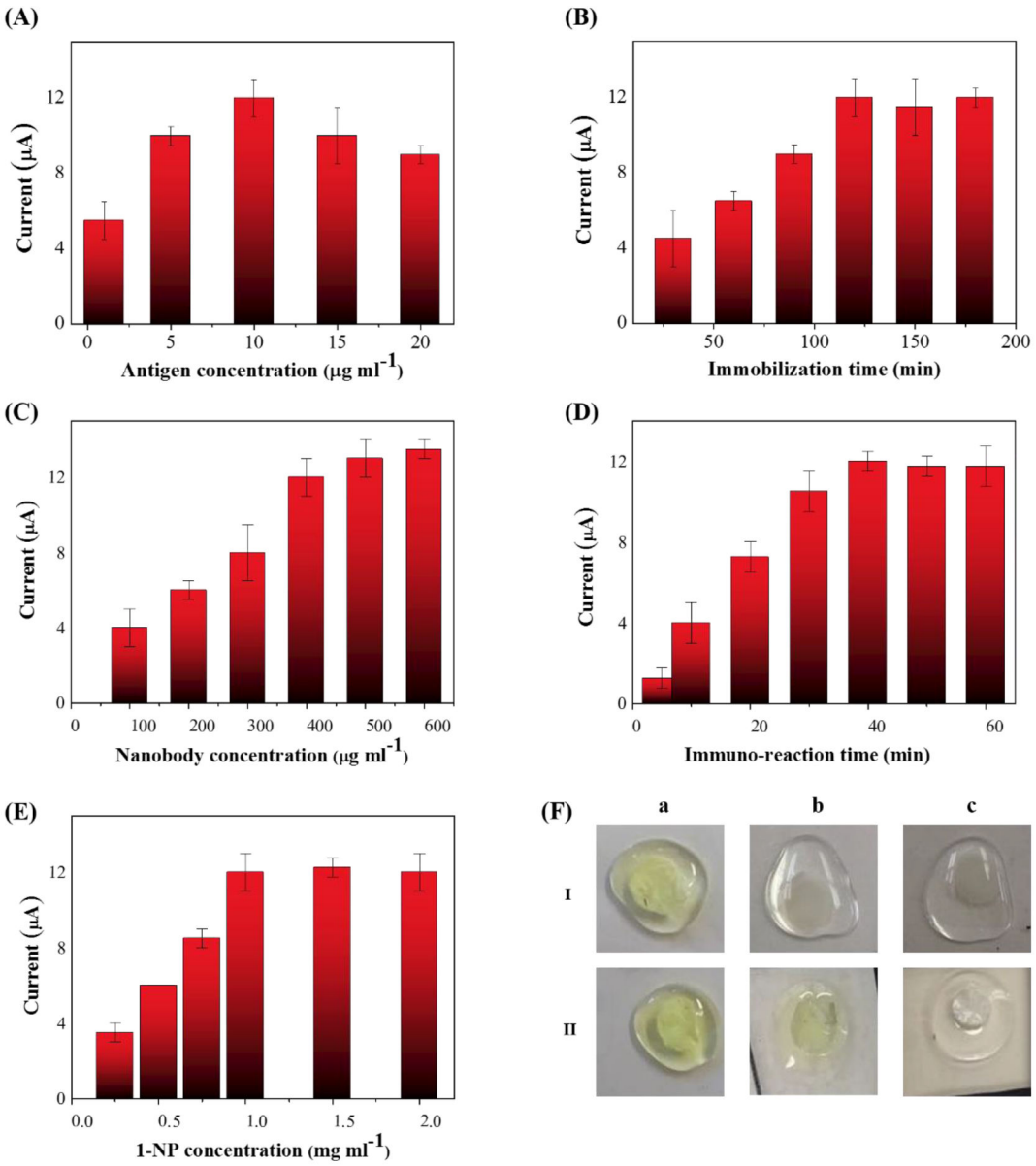

Figure 4:

Dependences of the obtained currents *via* DPV on: (A) antigen concentration, (B) antigen immobilization time, (C) nanobody concentration, (D) immuno-reaction time, (E) 1-NP concentration, (F) Blocking process of the active sites of (I) Ny CM and (II) NFM by: (a) control, (b) BSA and (c) EA, at concentration of 2%. *(n=3)*

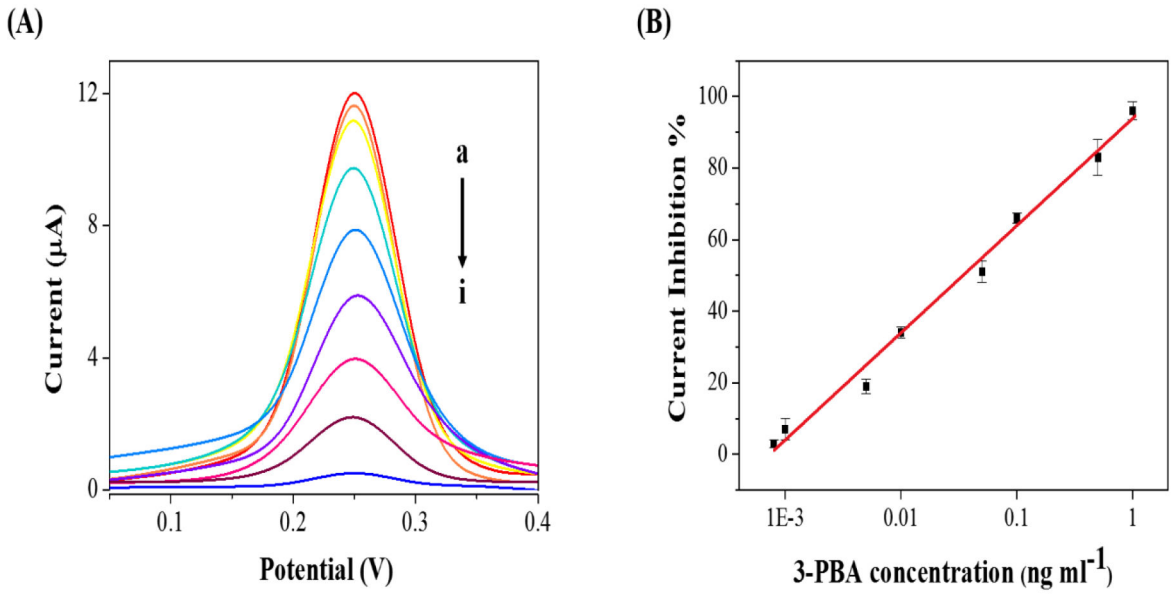

Figure 5:

(A) Electrocatalytic current responses of the assembled nanobody-based-electrochemical sensor for the detection of different concentrations of 3-PBA: 0 ng mL^{-1} (a), 0.0008 ng mL^{-1} (b), 0.001 ng mL^{-1} (c), 0.005 ng mL^{-1} (d), 0.01 ng mL^{-1} (e), 0.05 ng mL^{-1} (f), 0.1 ng mL^{-1} (g), 0.5 ng mL^{-1} (h) and 1 ng mL^{-1} (i); (**B**) Calibration curve of the immunosensor for the detection of different concentrations of 3-PBA. ($n = 3$).

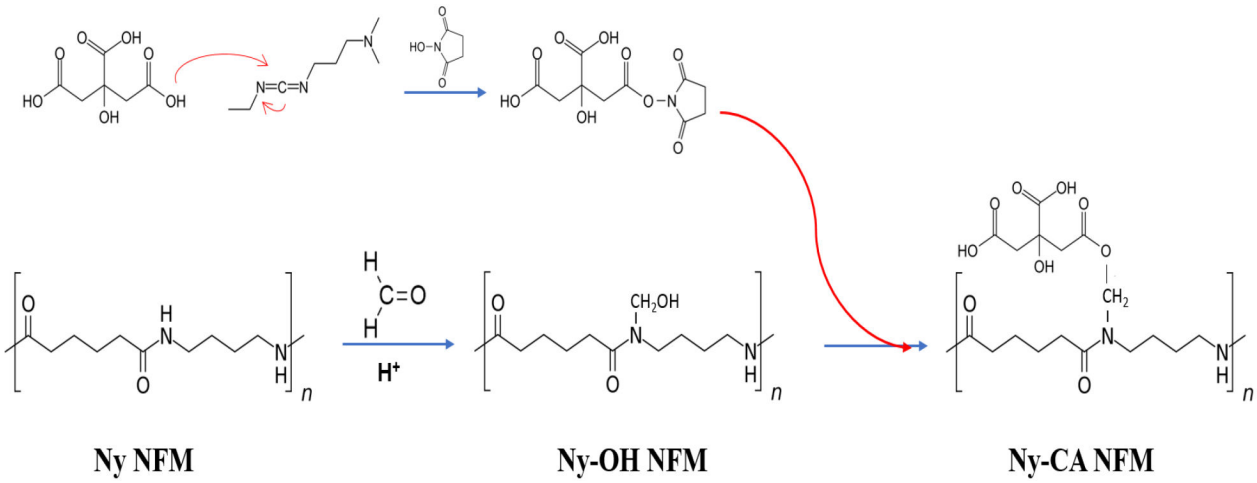

Scheme1:
Modification of Nylon NFM with citric acid

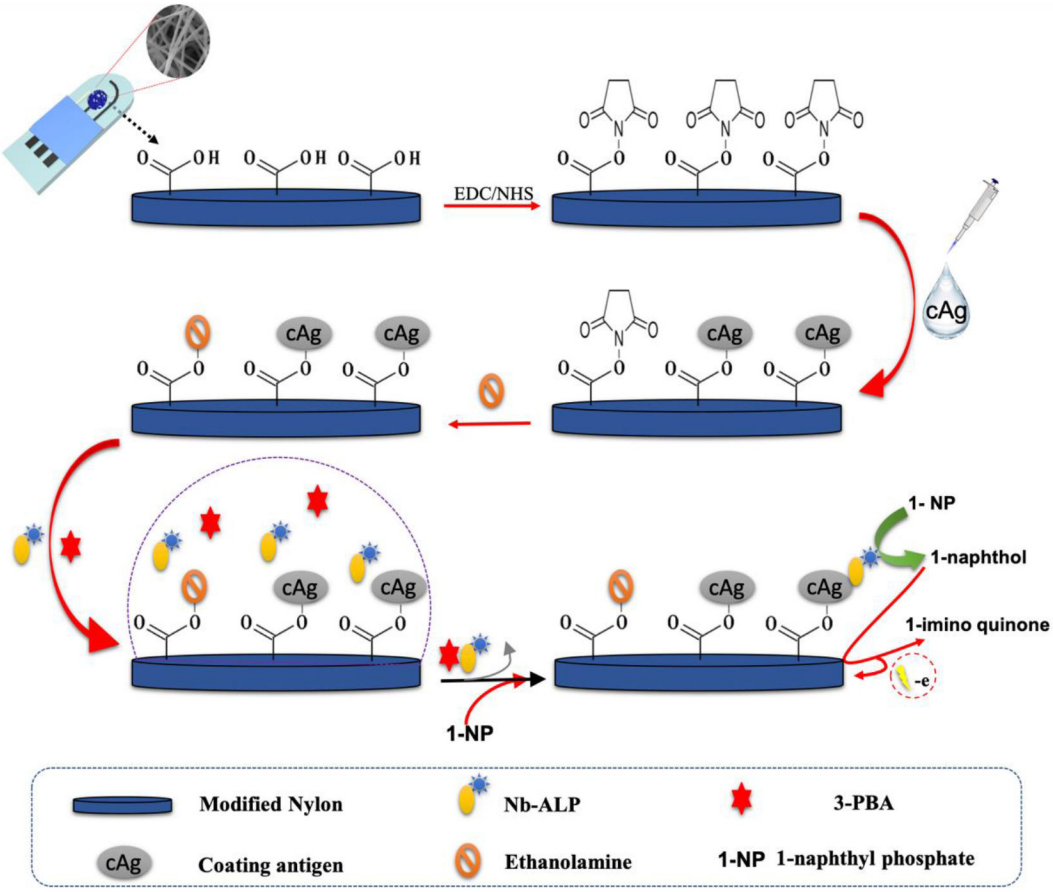

Scheme 2:

Fabrication process and sensing mechanism of nanobody-based-electrochemical immunosensor for 3-PBA detection

Table 1:

Comparison of the detection limits of 3-PBA of the developed nanosensor with other previously published researches:

	Method of detection	LOD (ng mL^{-1})	Ref.
1	polyclonal antibodies/ Enzyme-Linked Immunosorbent Assay	0.43	[13]
2	Mn-doped ZnS quantum dots (QDs)/ Optical sensor	25	[45]
3	Colloidal gold / monoclonal antibodies / Lateral flow immunoassay	130	[46]
4	HPLC-UV	130	[47]
5	Antibody fragments /Au electrode/ Electrochemical (EIS)	2.4	[48]
6	Bacteriophage-assisted sandwich immunoassay/ 11mercaptoundecanoic -Au electrode /Electrochemical (EIS)	740	[49]
7	Nb-ALP / Sensitive direct competitive fluorescence enzyme immunoassay (dc-FEIA)	0.011	[34]
8	Nb-ALP / Ny NFM-SPE/Electrochemical (DPV)	0.00064	This study

Table 2:

Cross-reactivity of the developed immunosensor for 3-PBA analogues and pyrethroids pesticides at 0.1 ng mL^{-1}.

Compound	3-phenoxybeneyl aldehyde	3-phenoxybenzyl alcohol	Permethrin	Cypermethrin	Deltamethrin
C.R%	12.9	0	0	0	0